






## Article

# Exact Solutions for the Sharma–Tasso–Olver Equation via the Sardar Subequation Method with a Comparison between Atangana Space–Time Beta-Derivatives and Classical Derivatives

Chanidaporn Pleumreedaporn <sup>1</sup>, Elvin J. Moore <sup>2,3,\*</sup>, Sekson Sirisubtawee <sup>2,3</sup>, Nattawut Khansai <sup>2</sup>  
and Songkran Pleumreedaporn <sup>1</sup>

- <sup>1</sup> Department of Mathematics, Faculty of Science and Technology, Rambhai Barni Rajabhat University, Chanthaburi 22000, Thailand; chanidaporn.p@rbru.ac.th (C.P.); songkran.p@rbru.ac.th (S.P.)  
<sup>2</sup> Department of Mathematics, Faculty of Applied Science, King Mongkut's University of Technology North Bangkok, Bangkok 10800, Thailand; sekson.s@sci.kmutnb.ac.th (S.S.); nattawut.khansai@gmail.com (N.K.)  
<sup>3</sup> Centre of Excellence in Mathematics, CHE, Si Ayutthaya Road, Bangkok 10400, Thailand  
\* Correspondence: elvin.j@sci.kmutnb.ac.th

**Abstract:** The Sharma–Tasso–Olver (STO) equation is a nonlinear, double-dispersive, partial differential equation that is physically important because it provides insights into the behavior of nonlinear waves and solitons in various physical areas, including fluid dynamics, optical fibers, and plasma physics. In this paper, the STO equation is generalized to a fractional equation by using Atangana (or Atangana–Baleanu) fractional space and time beta-derivatives since they have been found to be useful as a model for a variety of traveling-wave phenomena. Exact solutions are obtained for the integer-order and fractional-order equations by using the Sardar subequation method and an appropriate traveling-wave transformation. The exact solutions are obtained in terms of generalized trigonometric and hyperbolic functions. The exact solutions are derived for the integer-order STO and for a range of values of fractional orders. Numerical solutions are also obtained for a range of parameter values for both the fractional and integer orders to show some of the types of solutions that can occur. As examples, the solutions are obtained showing the physical behavior, such as the solitary wave solutions of the singular kink-type and periodic wave solutions. The results show that the Sardar subequation method provides a straightforward and efficient method for deriving new exact solutions for fractional nonlinear partial differential equations of the STO type.

**Keywords:** dispersive equation; fractional beta-derivative; traveling wave; soliton; kink-type solution

**MSC:** 35R11



**Citation:** Pleumreedaporn, C.; Moore, E.J.; Sirisubtawee, S.; Khansai, N.; Pleumreedaporn, S. Exact Solutions for the Sharma–Tasso–Olver Equation via the Sardar Subequation Method with a Comparison between Atangana Space–Time Beta-Derivatives and Classical Derivatives. *Mathematics* **2024**, *12*, 2155. <https://doi.org/10.3390/math12142155>

Academic Editor: Janusz Brzdęk

Received: 3 June 2024

Revised: 3 July 2024

Accepted: 8 July 2024

Published: 9 July 2024



**Copyright:** © 2024 by the authors. Licensee MDPI, Basel, Switzerland. This article is an open access article distributed under the terms and conditions of the Creative Commons Attribution (CC BY) license (<https://creativecommons.org/licenses/by/4.0/>).

## 1. Introduction

In this paper, the Sardar subequation method is used to obtain the exact solutions for the Sharma–Tasso–Olver equation defined by [1]

$$u_t + \alpha(u^3)_x + \frac{3}{2}\alpha(u^2)_{xx} + \alpha u_{xxx} = 0, \quad (1)$$

where  $u = u(x, t)$  is an unknown function of position  $x$  and time  $t$  and  $\alpha$  is a real parameter related to dispersion. This equation includes both a linear dispersive term  $\alpha u_{xxx}$  and the double nonlinear dispersive terms  $\alpha(u^3)_x$  and  $\alpha(u^2)_{xx}$ . The equation was proposed by Olver [1] in the development of a general method for finding evolution equations having infinitely many symmetries in which the Korteweg–de Vries, modified Korteweg–de Vries, Burgers', and sine-Gordon equations were generalized to have infinitely many symmetries.

Equation (1) can also be regarded as a member of the hierarchy of higher-order Burgers' equations [2].

In recent years, the STO equation has been studied by many physicists and mathematicians due to its appearance in traveling-wave applications, for example, in nonlinear optics [3], dispersive wave phenomena [4,5], plasma physics [5,6], conservation laws [7], Lie symmetry [8], nematic liquid crystals [9], and quantum field theory [10]. For a recent discussion in the literature on the many solution methods of the STO and related equations, see, e.g., Sirisubtawee et al. [11] and Sheikh et al. [12]. These solution methods include sine-cosine [13], exp-function [14], auxiliary equation [15], homotopy analysis [16], fractional complex transform [11,17], Darboux and Bäcklund transformations [18,19], improved  $(G'/G)$ -expansion [20],  $(-\phi(\xi))$ -expansion [21], modified multiple  $(G'/G)$ -expansion [22], fractional reduced differential transformation [23], improved fractional expansion [24], Khater [25], improved tanh-coth [26], direct algebraic [27,28], Hirota bilinear [29], truncated Painlevé expansion [30], multi-wave [31], the extension exponential rational function [32], novel  $(G'/G)$ -expansion [11], generalized Kudryashov [11], Fourier transform [33], the dynamical system [34,35], improved  $(G'/G)$ -expansion [36,37], Kudryashov [38], the modified simple equation method [12], modified F-expansion [39], and the complete discriminant system for the polynomial method [40].

In this paper, the Sardar subequation method is used to solve the STO equation because it has been shown to be a powerful and productive approach for solving a wide range of nonlinear evolution-type equations [41–49]. Some recent papers on the method and its applications that are closely related to the proposed work in this paper are as follows. Rezazadeh et al. [42] used the method to solve a variety of forms of  $(3 + 1)$ -dimensional Wazwaz–Benjamin–Bona–Mahony equations. Cinar et al. [46] used the method to derive exact soliton solutions for the perturbed Fokas–Lenells equation. Hussain et al. [50] used the method to obtain solutions of the conformable Klein–Gordon equation.

As discussed in more detail in Section 2, it is now well-known that fractional differential equations can often provide better models than integer-order equations for physical systems that include history or memory effects. In particular, the Atangana fractional beta-derivative [9,51] has been found to be useful because it is non-local and nonsingular and because it satisfies the chain rule of differentiation. It has also been found to have many useful applications in physical systems, including optical solitons, equal width wave propagation, unidirectional propagation of long waves, and monomode optical fibers [6,28,36,41,52–57].

The one-dimensional Sharma–Tasso–Olver equation with space–time beta-derivatives is as follows:

$$\frac{\partial^\gamma u}{\partial t^\gamma} + \alpha \frac{\partial^\beta u^3}{\partial x^\beta} + \frac{3}{2} \alpha \frac{\partial^\beta}{\partial x^\beta} \left( \frac{\partial^\beta u^2}{\partial x^\beta} \right) + \alpha \frac{\partial^\beta}{\partial x^\beta} \left( \frac{\partial^\beta}{\partial x^\beta} \left( \frac{\partial^\beta u}{\partial x^\beta} \right) \right) = 0, \quad (2)$$

where, for a water wave,  $u = u(x, t)$  usually represents a vertical surface displacement at position  $x$  and time  $t$  and  $\frac{\partial^\beta}{\partial x^\beta}(u(x, t))$  and  $\frac{\partial^\gamma}{\partial t^\gamma}(u(x, t))$  denote the beta partial derivatives defined in Section 2 with respect to  $x$  of order  $0 < \beta \leq 1$  and with respect to  $t$  of order  $0 < \gamma \leq 1$ , respectively.

The main purpose of this study is to derive exact traveling-wave solutions of Equations (1) and (2) using the Sardar subequation method and then to compare the solutions. The organization of this paper is as follows. In Section 2, a brief description is provided of the beta-derivative, its important characteristics, and its applications to a range of physical and engineering systems. In Section 3, the Sardar subequation method is applied to obtain the exact solutions of beta-derivative Equation (2) and classical integer-order STO Equation (1). Then, in Section 4, graphs of the numerical simulations are shown to illustrate the analytical results and to compare the beta-derivative and integer-derivative solutions. Finally, a discussion of the results is provided in Section 5, and the conclusions are provided in Section 6.

## 2. Atangana–Baleanu Beta-Derivative and Properties

As is well-known, many papers have now been published in which integer-order derivatives or integrals are replaced by fractional-order derivatives or integrals. There are now many fractional derivatives and integrals that have been developed for a wide range of different physical problems. Some examples of useful fractional derivatives include Riemann–Liouville [58], Caputo [58,59], Caputo–Fabrizio [60], Hadamard [61], Hilfer [62,63], Katugampala [64], and Hattaf [65,66].

### 2.1. Basic Properties of Atangana Beta-Derivative

In this section, some important properties of the Atangana or Atangana–Baleanu beta-derivative are summarized that are relevant for this paper. As noted previously, this derivative was initially proposed by Atangana and Baleanu [9,51] with the view of obtaining a fractional derivative that is both non-local and nonsingular. It also has the important property that it satisfies the chain rule of differentiation. The beta-derivative can be studied as a natural extension of the classical derivative to a fractional order, and most of its elementary properties are similar to the elementary properties of classical derivatives.

**Definition 1.** Let  $f$  be a function such that  $f : [0, \infty) \rightarrow \mathbb{R}$ . Then, the beta-derivative of  $f$  of order  $\beta$ , where  $0 < \beta \leq 1$ , is defined by [9,51,53,55–57]

$$D_t^\beta f(t) = \lim_{\varepsilon \rightarrow 0} \frac{f\left(t + \varepsilon\left(t + \frac{1}{\Gamma(\beta)}\right)^{1-\beta}\right) - f(t)}{\varepsilon}. \quad (3)$$

The basic properties of the beta-derivative are as follows [9,51,53,55–57]. Let  $f(t)$ ,  $g(t)$  be beta-differentiable functions for all  $t > 0$  and  $\beta \in (0, 1]$ .

- (1) If  $f$  is differentiable, then  $\lim_{\beta \rightarrow 1} D_t^\beta(f(t)) = \frac{df(t)}{dt}$ , i.e., the classical first derivative.
- (2)  $D_t^\beta(\lambda) = 0$ ,  $\forall \lambda \in \mathbb{R}$ .
- (3)  $D_t^\beta(af(t) + bg(t)) = aD_t^\beta f(t) + bD_t^\beta g(t)$ ,  $\forall a, b \in \mathbb{R}$ .
- (4)  $D_t^\beta(f(t)g(t)) = f(t)D_t^\beta g(t) + g(t)D_t^\beta f(t)$ .
- (5)  $D_t^\beta\left(\frac{f(t)}{g(t)}\right) = \frac{g(t)D_t^\beta f(t) - f(t)D_t^\beta g(t)}{(g(t))^2}$ , where  $g(t) \neq 0$ .
- (6) If  $f$  is differentiable, then  $D_t^\beta(f(t)) = \left(t + \frac{1}{\Gamma(\beta)}\right)^{1-\beta} \frac{df(t)}{dt}$ .
- (7) For a partial derivative, the definition is as follows:

$$\frac{\partial^\beta}{\partial t^\beta}(f(x, t)) = D_t^\beta(f(x, t)) = \lim_{\varepsilon \rightarrow 0} \frac{f\left(x, t + \varepsilon\left(t + \frac{1}{\Gamma(\beta)}\right)^{1-\beta}\right) - f(x, t)}{\varepsilon}.$$

**Theorem 1** ([9,51,53,55–57]). (Chain rule) Suppose  $f, g : (0, \infty) \rightarrow \mathbb{R}$  are differentiable and also beta-differentiable. Further, assume that  $g$  is a function defined in the range of  $f$ . Then, the beta-derivative of a composite function  $f \circ g$  can be written as

$$D_t^\beta(f \circ g)(t) = \left(t + \frac{1}{\Gamma(\beta)}\right)^{1-\beta} f'(g(t))g'(t), \quad (4)$$

where the prime symbol ( $'$ ) denotes the classical derivative.

### 2.2. Some Applications of Beta-Derivatives

In recent years, the beta-derivative [9,51] has been used in models for a number of important physical problems in nonlinear PDEs. Important reasons that it is useful are that, as noted previously, it is non-local and nonsingular and obeys the chain rule. In [53], the beta-derivative was applied to obtain a magnetic soliton solution for periodic wave propagation of a Heisenberg ferromagnetic spin chain in a  $(2 + 1)$ -dimensional nonlinear Schrödinger

equation (NLSE). The paper showed that the beta-derivative parameter significantly affects the rogue wave phenomena in this system and that the amplitudes and widths of such rogue waves are enlarged with the increase in  $\beta$ . The results are very helpful for analyzing the wave dynamics arising in many non-local and non-conservative/conservative physical systems. Another physical application of the beta-derivative discussed in [55] involved the space–time fractional modified equal width (FMEW) equation. This equation is related to the regularized long wave (RLW) equation and has solitary wave solutions with both positive and negative amplitudes but the same width. In this study, new traveling-wave solutions for the FMEW equation were constructed by using the unified method and varying the fractional orders. The new solutions were expressed in both polynomial and rational forms. In [67], the beta-derivative was used in a fractional optimal control analysis of COVID-19 and a dengue fever co-infection model. Further recent applications of the beta-derivative to physical systems include optical solitons, unidirectional propagation of long waves, and monomode optical fibers [6,28,36,41,52–57].

### 3. Exact Solutions of STO Equations by Sardar Subequation Method

In this section, the Sardar subequation method is used to derive exact solutions for beta-derivative Equation (2) and classical integer-order derivative Equation (1). The solution methods are based on the method provided in [50].

**Note:** To avoid confusion between the solutions of beta-derivative Equation (2) and classical integer-order derivative Equation (1), the notation  $b(x, t)$  is used for the solution of the beta-derivative equation and the notation  $u(x, t)$  is used for the solution of the classical equation.

#### 3.1. Atangana–Baleanu Beta-Derivative

Substituting  $b(x, t)$  for  $u(x, t)$ , Equation (2) becomes

$$\frac{\partial^\gamma b}{\partial t^\gamma} + \alpha \frac{\partial^\beta b^3}{\partial x^\beta} + \frac{3}{2} \alpha \frac{\partial^\beta}{\partial x^\beta} \left( \frac{\partial^\beta b^2}{\partial x^\beta} \right) + \alpha \frac{\partial^\beta}{\partial x^\beta} \left( \frac{\partial^\beta}{\partial x^\beta} \left( \frac{\partial^\beta b}{\partial x^\beta} \right) \right) = 0. \quad (5)$$

The first step in the Sardar method is to convert Equation (5) into an ordinary differential equation using the following fractional traveling-wave transformation

$$B(\xi) = b(x, t), \quad \xi = \frac{p}{\beta} \left( x + \frac{1}{\Gamma(\beta)} \right)^\beta + \frac{q}{\gamma} \left( t + \frac{1}{\Gamma(\gamma)} \right)^\gamma, \quad (6)$$

where  $p$  and  $q$  are nonzero constants that are related to the speed and direction of the wave and which will be found at a later step. Note that the space term in the traveling-wave transformation (6) corresponds to the beta-derivative with order  $\beta$  and the time term corresponds to the beta-derivative with order  $\gamma$ . The next step is to substitute Equation (6) into Equation (5) and then integrate the resulting equation with respect to  $\xi$  once to obtain the following ODE in the variable  $B = B(\xi)$ :

$$qB + \alpha p B^3 + 3\alpha p^2 B B' + \alpha p^3 B'' = 0, \quad (7)$$

where the prime notation ( $'$ ) represents the ordinary derivative of  $B(\xi)$  with respect to  $\xi$ .

It is then assumed that the solution form of (7) is

$$B(\xi) = \sum_{i=0}^N \omega_i \phi^i(\xi), \quad (8)$$

where  $\omega_i$ ,  $i = 0, 1, 2, \dots, N$  are constant coefficients to be determined at a later step and where the function  $\phi(\xi)$  satisfies the following auxiliary Equation (9):

$$\phi'(\xi) = \sqrt{\rho + a\phi^2(\xi) + \phi^4(\xi)}, \quad (9)$$

with  $a$  and  $\rho$  being real constants to be determined at a later step. Then, from the solution (8) and the homogeneous balance principle, i.e., by equating between the highest-order derivative and the highest-power nonlinear term in Equation (7), the value of  $N = 1$  is obtained, and hence the solution of (8) is of the form

$$B(\xi) = \omega_0 + \omega_1 \phi(\xi), \quad (10)$$

where  $\omega_0$  and  $\omega_1$  will be determined through steps of the Sardar subequation method.

Then, the Maple 17 package is used to obtain possible solutions for Equation (7) as follows. First, (10) along with its required derivatives from (9) are inserted into Equation (7). Then, the coefficients of  $\phi^i(\xi)$  (where  $i = 0, 1, 2, \dots, 6$ ) of the resulting polynomial are equated to zero and the following system of nonlinear algebraic equations in  $\omega_i$  ( $i = 0, 1$ ),  $p$ ,  $q$ , and  $\alpha$  is obtained:

$$\begin{aligned} \phi^0 : & 9p^4\omega_1^2\alpha^2\omega_0^2\rho - \alpha^2p^2\omega_0^6 - 2\alpha p\omega_0^4q - q^2\omega_0^2 = 0 \\ \phi^1 : & -2a\alpha^2p^4\omega_0^3\omega_1 + 18\alpha^2p^4\rho\omega_0\omega_1^3 - 6\alpha^2p^2\omega_0^5\omega_1 - 2a\alpha p^3q\omega_0\omega_1 - 8\alpha pq\omega_0^3\omega_1 \\ & - 2q^2\omega_0\omega_1 = 0 \\ \phi^2 : & -a^2\alpha^2p^6\omega_1^2 + 3a\alpha^2p^4\omega_0^2\omega_1^2 + 9\alpha^2p^4\rho\omega_1^4 - 15\alpha^2p^2\omega_0^4\omega_1^2 - 2a\alpha p^3q\omega_1^2 \\ & - 12\alpha pq\omega_0^2\omega_1^2 - q^2\omega_1^2 = 0 \\ \phi^3 : & 12a\alpha^2p^4\omega_0\omega_1^3 - 4\alpha^2p^4\omega_0^3\omega_1 - 20\alpha^2p^2\omega_0^3\omega_1^3 - 4\alpha p^3q\omega_0\omega_1 - 8\alpha pq\omega_0\omega_1^3 = 0 \\ \phi^4 : & -4a\alpha^2p^6\omega_1^2 + 7a\alpha^2p^4\omega_1^4 - 3\alpha^2p^4\omega_0^2\omega_1^2 - 15\alpha^2p^2\omega_0^2\omega_1^4 - 4\alpha p^3q\omega_1^2 \\ & - 2\alpha pq\omega_1^4 = 0 \\ \phi^5 : & 6\alpha^2p^4\omega_0\omega_1^3 - 6\alpha^2p^2\omega_0\omega_1^5 = 0 \\ \phi^6 : & -4\alpha^2p^6\omega_1^2 + 5\alpha^2p^4\omega_1^4 - \alpha^2p^2\omega_1^6 = 0 \end{aligned} \quad (11)$$

Then, the Maple 17 software package provides only set of solutions of system (11) as follows:

$$a = \frac{2q}{\alpha p^3}, \rho = \frac{q^2}{\alpha^2 p^6}, \omega_0 = 0, \omega_1 = -p, \quad (12)$$

where  $\alpha > 0$  is the dispersive constant and  $p$  and  $q$  are arbitrary constants with  $p, q \neq 0$ . In consequence, the exact solutions of Equation (10) corresponding to Equation (12) are as follows.

Case 1: If  $a < 0$  and  $\rho = 0$ , then there are no exact solutions  $b_{1,2}^\pm(x, t)$  because, by (12), if  $\rho = 0$ , then  $a$  must be zero, which contradicts the condition that  $a < 0$ .

Case 2: If  $a > 0$  and  $\rho = 0$ , then there are no exact solutions  $b_{3,4}^\pm(x, t)$  because, by (12), if  $\rho = 0$ , then  $a$  must be zero, which contradicts the condition that  $a > 0$ .

From (12), the value of  $\rho$  is  $\rho = \frac{q^2}{\alpha^2 p^6}$ . Therefore, by the Sardar subequation method and algebraic manipulations, it is found that the only solutions of (10) are as follows.

Case 3: If  $a < 0$  and  $\rho = \frac{q^2}{\alpha^2 p^6}$ , then the exact traveling-wave solutions are

$$b_5(x, t) = p\sqrt{-\frac{a}{2}} \tanh_{mn} \left( \sqrt{-\frac{a}{2}} \xi \right), \quad (13)$$

$$b_6(x, t) = p\sqrt{-\frac{a}{2}} \coth_{mn} \left( \sqrt{-\frac{a}{2}} \xi \right), \quad (14)$$

$$b_7^\pm(x, t) = p\sqrt{-\frac{a}{2}} \left( \tanh_{mn} \left( \sqrt{-2a\xi} \right) \pm i\sqrt{mn} \operatorname{sech}_{mn} \left( \sqrt{-2a\xi} \right) \right), \quad (15)$$

$$b_8^\pm(x, t) = p\sqrt{-\frac{a}{2}}\left(\coth_{mn}\left(\sqrt{-2a}\xi\right) \pm \sqrt{mn}\operatorname{csch}_{mn}\left(\sqrt{-2a}\xi\right)\right), \quad (16)$$

$$b_9(x, t) = p\sqrt{-\frac{a}{8}}\left(\tanh_{mn}\left(\sqrt{-\frac{a}{8}}\xi\right) + \coth_{mn}\left(\sqrt{-\frac{a}{8}}\xi\right)\right), \quad (17)$$

where

$$\xi = \frac{p}{\beta}\left(x + \frac{1}{\Gamma(\beta)}\right)^\beta + \frac{q}{\gamma}\left(t + \frac{1}{\Gamma(\gamma)}\right)^\gamma \quad (18)$$

and

$$\begin{aligned} \operatorname{sech}_{mn}(\xi) &= \frac{2}{me^\xi + ne^{-\xi}}, & \operatorname{csch}_{mn}(\xi) &= \frac{2}{me^\xi - ne^{-\xi}}, \\ \tanh_{mn}(\xi) &= \frac{me^\xi - ne^{-\xi}}{me^\xi + ne^{-\xi}}, & \coth_{mn}(\xi) &= \frac{me^\xi + ne^{-\xi}}{me^\xi - ne^{-\xi}}. \end{aligned} \quad (19)$$

Case 4: If  $a > 0$  and  $\rho = \frac{q^2}{\alpha^2 p^6}$ , then the exact traveling-wave solutions are

$$b_{10}(x, t) = -p\sqrt{\frac{a}{2}}\tan_{mn}\left(\sqrt{\frac{a}{2}}\xi\right), \quad (20)$$

$$b_{11}(x, t) = p\sqrt{\frac{a}{2}}\cot_{mn}\left(\sqrt{\frac{a}{2}}\xi\right), \quad (21)$$

$$b_{12}^\pm(x, t) = -p\sqrt{\frac{a}{2}}\left(\tan_{mn}\left(\sqrt{2a}\xi\right) \pm \sqrt{mn}\sec_{mn}\left(\sqrt{2a}\xi\right)\right), \quad (22)$$

$$b_{13}^\pm(x, t) = p\sqrt{\frac{a}{2}}\left(\cot_{mn}\left(\sqrt{2a}\xi\right) \pm \sqrt{mn}\csc_{mn}\left(\sqrt{2a}\xi\right)\right), \quad (23)$$

$$b_{14}(x, t) = -p\sqrt{\frac{a}{8}}\left(\tan_{mn}\left(\sqrt{\frac{a}{8}}\xi\right) - \cot_{mn}\left(\sqrt{\frac{a}{8}}\xi\right)\right), \quad (24)$$

where

$$\xi = \frac{p}{\beta}\left(x + \frac{1}{\Gamma(\beta)}\right)^\beta + \frac{q}{\gamma}\left(t + \frac{1}{\Gamma(\gamma)}\right)^\gamma \quad (25)$$

and

$$\begin{aligned} \sec_{mn}(\xi) &= \frac{2}{me^{i\xi} + ne^{-i\xi}}, & \csc_{mn}(\xi) &= \frac{2i}{me^{i\xi} - ne^{-i\xi}}, \\ \tan_{mn}(\xi) &= -i\frac{me^{i\xi} - ne^{-i\xi}}{me^{i\xi} + ne^{-i\xi}}, & \cot_{mn}(\xi) &= i\frac{me^{i\xi} + ne^{-i\xi}}{me^{i\xi} - ne^{-i\xi}}, \end{aligned} \quad (26)$$

As a final check, substitution of the functions in Equations (13)–(24) into Maple 17 showed that the functions are exact solutions of the original Equation (5).

### 3.2. Integer-Order Derivative

The solution for the integer-order derivative is similar to the solution for the beta-derivative except for the initial assumption for the traveling-wave transformation (6). The solution is again based on Hussain et al. [50].

In this case, the traveling-wave transform is assumed to be

$$U(\xi) = u(x, t), \quad \text{and} \quad \xi = x - ct, \quad (27)$$

where  $c$  is the wave speed, which can be positive for waves traveling in the positive  $x$ -direction or negative for waves traveling in the negative  $x$ -direction. Then, substitution of Equation (27) into the Sharma–Tasso–Olver Equation (1) provides the ODE:

$$-cU' + \alpha(U^3)' + \frac{3}{2}\alpha(U^2)'' + \alpha U''' = 0, \quad (28)$$

where the prime notation ( $'$ ) represents the ordinary derivative with respect to  $\xi$ .

Then, after integration of Equation (28) with respect to the variable  $\xi$  and assuming a zero constant of integration, the following nonlinear ordinary differential equation for the function  $U$  is obtained:

$$-cU + \alpha U^3 + 3\alpha U U' + \alpha U'' = 0. \quad (29)$$

As in Equation (10), it is assumed that the solution form of (29) is

$$U(\xi) = \sum_{i=0}^N \omega_i \phi^i(\xi). \quad (30)$$

As for the fractional case, the homogeneous balance principle, i.e., equating between the highest-order derivative and the highest-power nonlinear term in Equation (29), provides the value  $N = 1$ , and therefore the solution of (30) is of the form

$$U(\xi) = \omega_0 + \omega_1 \phi(\xi), \quad (31)$$

where  $\omega_0$  and  $\omega_1$  will be determined through steps of the Sardar subequation method.

Then, Maple 17 can be used to solve (31) as follows. First, Equation (31) along with its required derivatives from (9) are substituted into (29) and then the coefficients of  $\phi^i(\xi)$  (where  $i = 0, 1, 2, \dots, 6$ ) of the resulting polynomial are set to zero. The following system of nonlinear algebraic equations in  $\omega_i (i = 0, 1), c, \alpha, \rho$  is then obtained:

$$\begin{aligned} \phi^0 : & -\alpha^2 \omega_0^6 + 9\alpha^2 \omega_1^2 \omega_0^2 \rho + 2c\omega_0^4 \alpha - c^2 \omega_0^2 = 0 \\ \phi^1 : & -6\alpha^2 \omega_0^5 \omega_1 - 2\alpha^2 \omega_0^3 \omega_1 + 18\alpha^2 \rho \omega_0 \omega_1^3 + 8\alpha c \omega_0^3 \omega_1 + 2\alpha \alpha c \omega_0 \omega_1 \\ & - 2c^2 \omega_0 \omega_1 = 0 \\ \phi^2 : & -15\alpha^2 \omega_0^4 \omega_1^2 + 3\alpha^2 \omega_0^2 \omega_1^2 + 9\alpha^2 \rho \omega_1^4 - \alpha^2 \alpha^2 \omega_1^2 + 12\alpha c \omega_0^2 \omega_1^2 + 2\alpha \alpha c \omega_1^2 \\ & - c^2 \omega_1^2 = 0 \\ \phi^3 : & -20\alpha^2 \omega_0^3 \omega_1^3 + 12\alpha \alpha^2 \omega_0 \omega_1^3 - 4\alpha^2 \omega_0^3 \omega_1 + 8\alpha c \omega_0 \omega_1^3 + 4\alpha c \omega_0 \omega_1 = 0 \\ \phi^4 : & -15\alpha^2 \omega_0^2 \omega_1^4 + 7\alpha \alpha^2 \omega_1^4 - 3\alpha^2 \omega_0^2 \omega_1^2 + 2\alpha c \omega_1^4 - 4\alpha \alpha^2 \omega_1^2 + 4\alpha c \omega_1^2 = 0 \\ \phi^5 : & -6\alpha^2 \omega_0 \omega_1^5 + 6\alpha^2 \omega_0 \omega_1^3 = 0 \\ \phi^6 : & -\alpha^2 \omega_1^6 + 5\alpha^2 \omega_1^4 - 4\alpha^2 \omega_1^2 = 0 \end{aligned} \quad (32)$$

Then, the Maple 17 software package provides only one set of solutions of system (32) as follows:

$$a = -\frac{1}{2} \frac{c}{\alpha}, \quad \rho = \frac{1}{16} \frac{c^2}{\alpha^2}, \quad \omega_0 = 0, \quad \omega_1 = 2, \quad (33)$$



where  $\alpha > 0$  is the dispersive constant and the wave speed  $c$  is an arbitrary constant that can be positive or negative. In consequence, the exact solutions of Equation (31) corresponding to Equation (33) are as follows.

Case 1: If  $a < 0$  and  $\rho = 0$ , then there are no exact solutions  $u_{1,2}^{\pm}(x, t)$  because, by (33), if  $\rho = 0$ , then  $a$  must be zero, which contradicts the condition that  $a < 0$ .

Case 2: If  $a > 0$  and  $\rho = 0$ , then there are no exact solutions  $u_{3,4}^{\pm}(x, t)$  because, by (33), if  $\rho = 0$ , then  $a$  must be zero, which contradicts the condition that  $a > 0$ .

From (33),  $\rho = \frac{1}{16} \frac{c^2}{a^2}$ . Therefore, by the Sardar subequation method and algebraic manipulations, the only solutions of (31) are as follows.

Case 3: If  $a < 0$ , i.e.,  $c > 0$ , and  $\rho = \frac{1}{16} \frac{c^2}{a^2}$ , then the exact traveling-wave solutions are

$$u_5(x, t) = 2\sqrt{-\frac{a}{2}} \tanh_{mn} \left( \sqrt{-\frac{a}{2}} \xi \right), \quad (34)$$

$$u_6(x, t) = 2\sqrt{-\frac{a}{2}} \coth_{mn} \left( \sqrt{-\frac{a}{2}} \xi \right), \quad (35)$$

$$u_7^{\pm}(x, t) = 2\sqrt{-\frac{a}{2}} \left( \tanh_{mn} \left( \sqrt{-2a} \xi \right) \pm i\sqrt{mn} \operatorname{sech}_{mn} \left( \sqrt{-2a} \xi \right) \right), \quad (36)$$

$$u_8^{\pm}(x, t) = 2\sqrt{-\frac{a}{2}} \left( \coth_{mn} \left( \sqrt{-2a} \xi \right) \pm \sqrt{mn} \operatorname{csch}_{mn} \left( \sqrt{-2a} \xi \right) \right), \quad (37)$$

$$u_9(x, t) = 2\sqrt{-\frac{a}{8}} \left( \tanh_{mn} \left( \sqrt{-\frac{a}{8}} \xi \right) + \coth_{mn} \left( \sqrt{-\frac{a}{8}} \xi \right) \right), \quad (38)$$

where  $\xi = x - ct$ .

Case 4: If  $a > 0$ , i.e.,  $c < 0$ , and  $\rho = \frac{1}{16} \frac{c^2}{a^2}$ , then the exact traveling-wave solutions are

$$u_{10}(x, t) = -2\sqrt{\frac{a}{2}} \tan_{mn} \left( \sqrt{\frac{a}{2}} \xi \right), \quad (39)$$

$$u_{11}(x, t) = 2\sqrt{\frac{a}{2}} \cot_{mn} \left( \sqrt{\frac{a}{2}} \xi \right), \quad (40)$$

$$u_{12}^{\pm}(x, t) = -2\sqrt{\frac{a}{2}} \left( \tan_{mn} \left( \sqrt{2a} \xi \right) \pm \sqrt{mn} \sec_{mn} \left( \sqrt{2a} \xi \right) \right), \quad (41)$$

$$u_{13}^{\pm}(x, t) = 2\sqrt{\frac{a}{2}} \left( \cot_{mn} \left( \sqrt{2a} \xi \right) \pm \sqrt{mn} \csc_{mn} \left( \sqrt{2a} \xi \right) \right), \quad (42)$$

$$u_{14}(x, t) = -2\sqrt{\frac{a}{8}} \left( \tan_{mn} \left( \sqrt{\frac{a}{8}} \xi \right) - \cot_{mn} \left( \sqrt{\frac{a}{8}} \xi \right) \right), \quad (43)$$

where  $\xi = x - ct$ .

As for the fractional solutions, it has been checked that the functions in Equations (34)–(43) are exact solutions of the original Equation (1) by substituting them in Maple 17 and finding



that they satisfy Equation (1). The integer-order solutions should also be obtained from the  $\beta$ -derivative solutions in the limits as the fractional orders  $\beta \rightarrow 1, \gamma \rightarrow 1$ .

#### 4. Graphical Results

In this section, graphs are plotted of some interesting exact traveling-wave solutions of the beta-derivative Sharma–Tasso–Olver Equation (5) and classical derivative STO Equation (1). In particular, graphs are plotted for Case 3 ( $a < 0$ ) in Figures 1 and 2 and for Case 4 ( $a > 0$ ) in Figures 3 and 4. For both cases, the exact solutions are plotted through 3D, 2D, and contour plots for the following range of fractional-order values:  $\gamma = 1, 0.8, 0.6$ , and  $\beta = 0.8$ . The exact traveling-wave solutions  $b_8^+(x, t)$  in Equation (16),  $b_{12}^+(x, t)$  in Equation (22), have been selected to show how their physical behavior changes when the values of the fractional time-order  $\gamma$  are varied. All figures were plotted with the Maple software package.

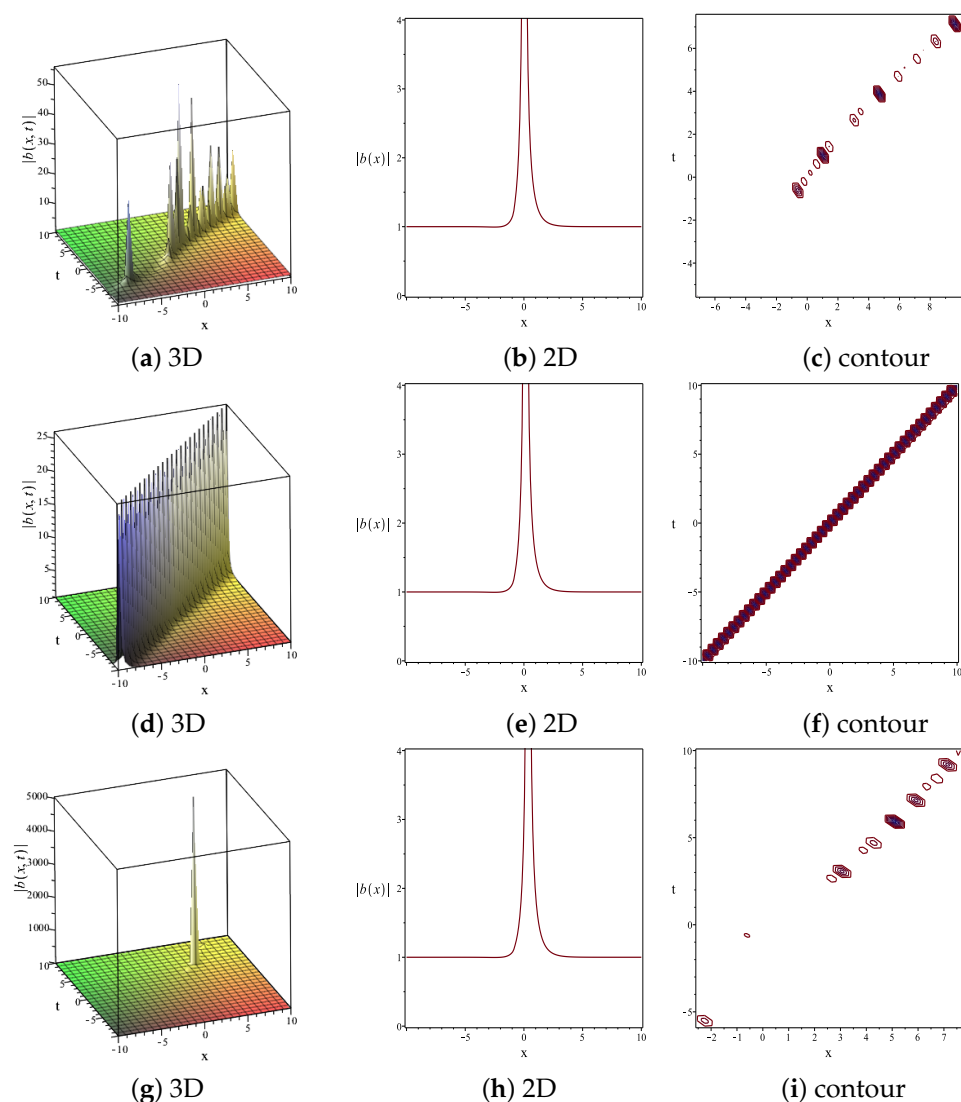


**Figure 1.** Graphs of magnitudes obtained utilizing the Sardar subequation method for beta-derivatives: (a–c) show  $\gamma = 1, \beta = 0.8, b_8^+(x, t)$  in (16); (d–f) show  $\gamma = 0.8, \beta = 0.8, b_8^+(x, t)$  in (16); (g–i) show  $\gamma = 0.6, \beta = 0.8, b_8^+(x, t)$  in (16).

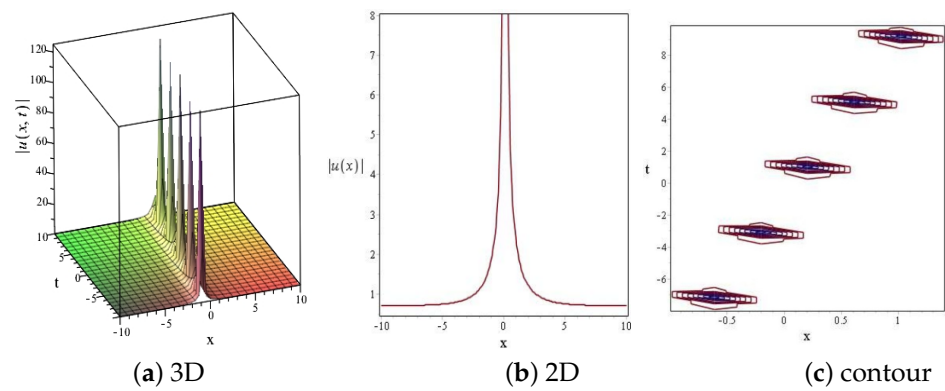


**Figure 2.** Graphs of magnitudes obtained utilizing the Sardar subequation method for classical derivatives: (a–c) show  $c = 0.1$ ,  $u_8^+(x, t)$  in (37).

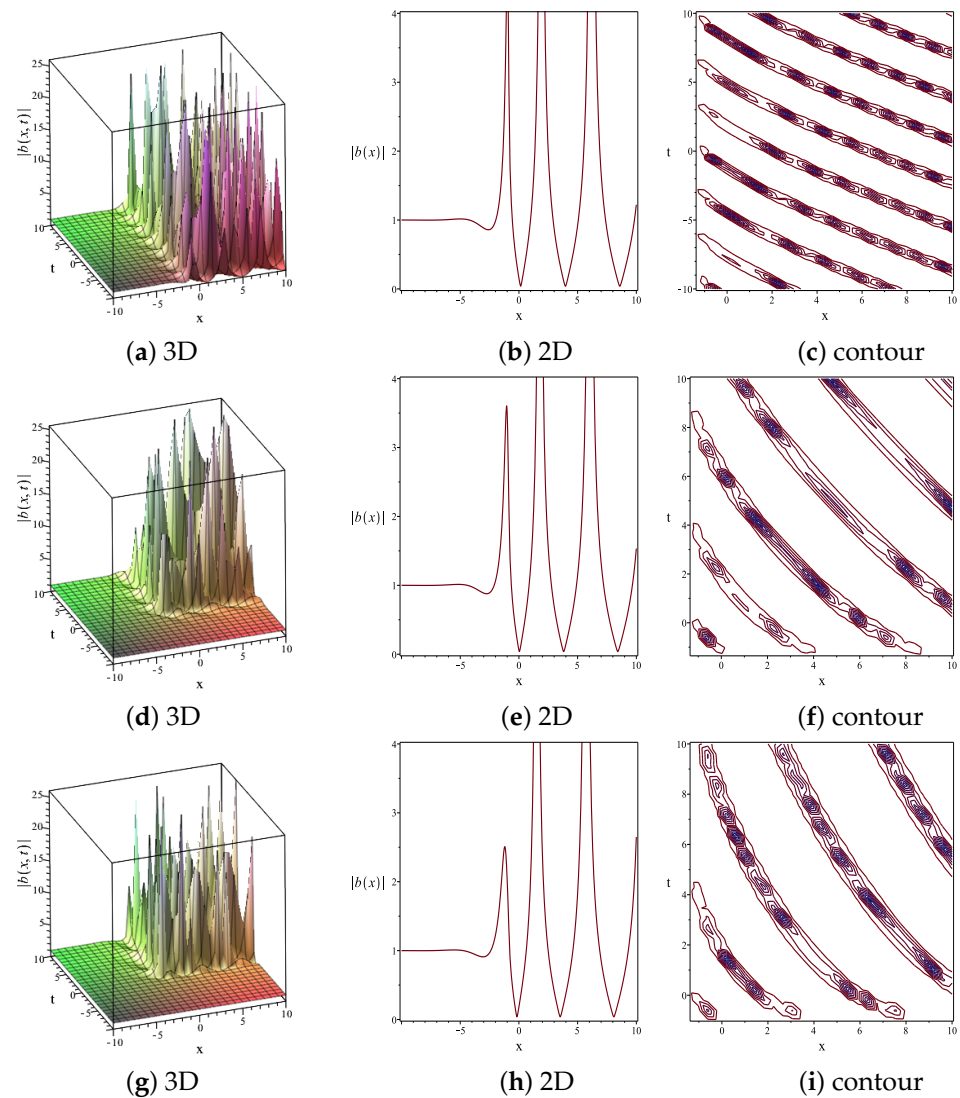


**Figure 3.** Graphs of magnitudes obtained utilizing the Sardar subequation method for beta-derivatives: (a–c) show  $\gamma = 1$ ,  $\beta = 0.8$ ,  $b_{12}^+(x, t)$  in (22); (d–f) show  $\gamma = 0.8$ ,  $\beta = 0.8$ ,  $b_{12}^+(x, t)$  in (22); (g–i) show  $\gamma = 0.6$ ,  $\beta = 0.8$ ,  $b_{12}^+(x, t)$  in (22).

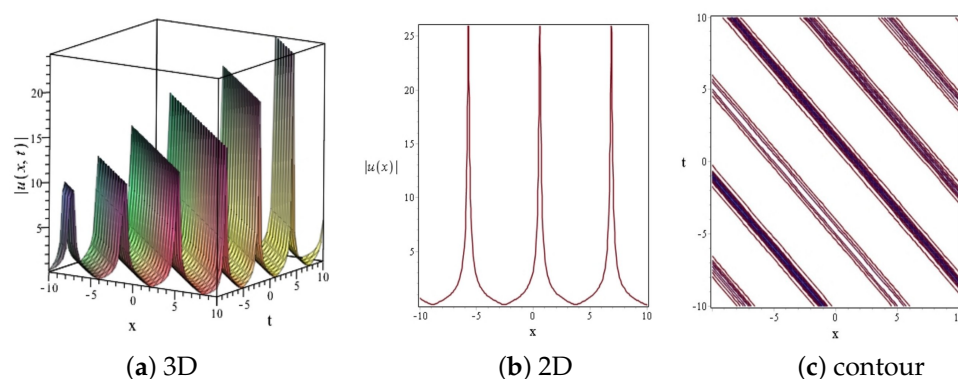


**Figure 4.** Graphs of magnitudes obtained utilizing the Sardar subequation method for classical derivatives: (a–c) show  $c = -1$ ,  $u_{12}^+(x, t)$  in (41).

In Figure 1a–i magnitudes of the exact solutions for the beta-derivative  $b_8^+(x, t)$  in (16) are plotted as 3D, 2D, and contour plots for the following parameter values:  $m = 1.2, n = 1.4, p = 1, q = -1$ , and  $\alpha = 1$  calculated at the following sets of fractional orders  $\{\gamma = 1, \beta = 0.8\}$ ,  $\{\gamma = 0.8, \beta = 0.8\}$ , and  $\{\gamma = 0.6, \beta = 0.8\}$ , respectively. For comparison, Figure 2a–c show the magnitudes of the exact solutions for the classical-order  $u_8^+(x, t)$  in (37) plotted as 3D, 2D, and contour plots for the following parameter values:  $m = 1.2, n = 1.4, c = 0.1$ , and  $\alpha = 0.2$ . As can be seen from the 3D graphs of Figures 1 and 2, the physical behavior of  $|b_8^+(x, t)|$  and  $|u_8^+(x, t)|$  can be classified as a singular kink-type wave. It can also be seen that the main effect of changing the fractional orders is to move the positions of the singularities in the solitary waves. It can also be seen clearly from the contour plots that the waves are traveling to the right since  $x$  is increasing with  $t$ . This corresponds to a positive wave speed  $\frac{p}{q} < 0$  for the fractional waves and  $c > 0$  for the integer-order waves.

In Figure 3a–i magnitudes of the exact solutions for the beta-derivative  $b_{12}^+(x, t)$  in (22) are plotted as 3D, 2D, and contour plots for the following parameter values:  $m = 1.2, n = 1.4, p = 1, q = 1$ , and  $\alpha = 1$  calculated at the following sets of fractional orders  $\{\gamma = 1, \beta = 0.8\}$ ,  $\{\gamma = 0.8, \beta = 0.8\}$ , and  $\{\gamma = 0.6, \beta = 0.8\}$ , respectively. In Figure 4a–c, magnitudes of the exact solutions for the classical-order  $u_{12}^+(x, t)$  in (41) are plotted as 3D, 2D, and contour plots for the following parameter values:  $m = 1.2, n = 1.4, c = -1$ , and  $\alpha = 1$ . The 3D graphs of Figures 3 and 4, the physical behavior of  $|b_{12}(x, t)|$  and  $|u_{12}(x, t)|$ , can be classified as a periodic wave. In this case, it can also be seen clearly from the contour plots that the waves are traveling to the left since  $x$  is decreasing with  $t$ . This corresponds to a negative wave speed  $\frac{p}{q} > 0$  for the fractional waves and  $c < 0$  for the integer-order waves.

## 5. Discussion of Results

In this paper, the Sardar subequation method has been used to obtain exact traveling-wave solutions of the STO Equation (2) with Atangana fractional space and time beta-derivatives and the classical STO Equation (1) with integer derivatives. Using this method, and with the aid of the Maple 17 software package, the exact solutions of the equations have been obtained in terms of the special generalized hyperbolic and trigonometric functions defined in Equations (19) and (26). These exact traveling-wave solutions for Equations (1) and (2) have been successfully obtained by the method because the traveling-wave transformation was appropriately selected as expressed in (6) for the beta-derivative and (27) for the integer order and chain rule of the beta-derivative, which exist as described in Section 2.1. It is worth noting that regular hyperbolic and trigonometric function solutions for Equations (1) and (2) are always derived when the Sardar subequation method is applied for the problems. This is because the special generalized hyperbolic and trigonometric function solutions generated by the used method can be reduced to the regular hyperbolic

and trigonometric functions by selecting  $m = n = 1$ . The Maple package has been used to plot 3D, 2D, and contour plots of the magnitude of the selected solutions for a range of values of fractional orders  $\beta$  and  $\gamma$  in order to explore their effects on the physical behavior of the selected solutions. From the results, two of the exact solutions of Equation (2) have been found with different physical behavior, namely a singular kink-type wave solution and a periodic wave solution. In each case, the main effect of changing the value of  $\beta$  was to move the positions of the singularities. In each case, it was found that the beta-derivative and integer-order solutions were of a similar type but with differences in their details. As stated at the end of Section 3, it has been verified that all the solutions in Section 3 are exact solutions of Equations (2) or (1) by substituting them back into the original equation with the assistance of Maple.

## 6. Conclusions

In this paper, it has been shown that, with the aid of the computer package Maple, the Sardar subequation method is a powerful and reliable technique for obtaining exact nonlinear traveling-wave solutions of both integer-order and fractional-order nonlinear evolution equations of the STO type. Furthermore, an application of the method is simpler and more straightforward than other existing methods such as the  $(G'/G, 1/G)$ -expansion method [68] because its associated auxiliary Equation (9) is a first-order nonlinear differential equation. It is therefore easier to solve to obtain analytical solutions than the complicated system of auxiliary equations of the  $(G'/G, 1/G)$ -expansion method. Finally, it has been found that many PDEs equipped with the Atangana beta-derivative can be analytically solved for exact traveling-wave solutions because the derivative has the chain rule property and can be written in terms of the first-order derivative when the required condition exists. With this advantage, integrable PDEs in the sense of such a derivative can be reduced to an ordinary differential equation with the aid of the fractional traveling-wave transformation. Possible future work would be to examine in considerably more detail the types of solutions that can be obtained from the Atangana fractional beta-derivative model of the STO equation and to compare the solutions obtained in this paper with data from real physical systems. The results obtained in this paper suggest that the Sardar subequation method could potentially be applied to other PDEs with Atangana–Baleanu fractional beta-derivatives.

**Author Contributions:** Conceptualization, C.P. and S.P.; methodology, C.P., E.J.M. and N.K.; software, C.P., N.K. and S.P.; validation, C.P., E.J.M. and S.S.; formal analysis, C.P., E.J.M. and S.S.; writing—original draft preparation, C.P., E.J.M. and S.S.; writing—review and editing, C.P., E.J.M. and S.S.; supervision, C.P., E.J.M. and S.S. All authors have read and agreed to the published version of the manuscript.

**Funding:** The authors have received no funding for this research.

**Data Availability Statement:** The Maple 17 programs used to obtain the results in this research can be obtained by application to Dr. Chanidaporn Pleumpreedaporn through her email address.

**Acknowledgments:** The authors wish to thank the anonymous reviewers for their very helpful suggestions regarding this manuscript.

**Conflicts of Interest:** The authors declare no conflicts of interest.

## Abbreviations

The following abbreviations are used in this manuscript:

MDPI	Multidisciplinary Digital Publishing Institute
PDE	Partial differential equation
STO	Sharma–Tasso–Olver
2D	Two dimensions
3D	Three dimensions

## References

- Olver, P. Evolution equations possessing infinitely many symmetries. *J. Math. Phys.* **1977**, *18*, 1212–1215. [\[CrossRef\]](#)
- Wang, M. Higher Burgers equation. *Acta Math. Sci.* **1986**, *6*, 355–360. [\[CrossRef\]](#)
- Pavani, K.; Raghavendar, K.; Aruna, K. Soliton solutions of the time-fractional Sharma–Tasso–Olver equations arise in nonlinear optics. *Opt. Quantum Electron.* **2024**, *56*, 748. [\[CrossRef\]](#)
- Khan, K.; Koppelaar, H.; Akbar, M.; Mohyud-Din, S. Analysis of travelling wave solutions of double dispersive Sharma–Tasso–Olver equation. *J. Ocean Eng. Sci.* **2022**, *3*, 18. [\[CrossRef\]](#)
- Akbar, M.A.; Abdullah, F.A.; Kumar, S.; Khaled, A.G. Assorted soliton solutions to the nonlinear dispersive wave models in inhomogeneous media. *Results Phys.* **2022**, *39*, 105720. [\[CrossRef\]](#)
- Seadawy, A.R.; Nasreen, N.; Lu, D.; Arshad, M. Arising wave propagation in nonlinear media for the  $(2 + 1)$ -dimensional Heisenberg ferromagnetic spin chain dynamical model. *Physica A Stat. Mech. Appl.* **2020**, *538*, 122846. [\[CrossRef\]](#)
- Johnpillai, A.; Khalique, C. On the solutions and conservation laws for the Sharma–Tasso–Olver equation. *Sci. Asia* **2014**, *40*, 451–455. [\[CrossRef\]](#)
- Kumar, S.; Khan, I.; Rani, S.; Ghanbari, B. Lie symmetry analysis and dynamics of exact solutions of the  $(2 + 1)$ -dimensional nonlinear Sharma–Tasso–Olver equation. *Math. Probl. Eng.* **2021**, *2021*, 9961764. [\[CrossRef\]](#)
- Atangana, A.; Baleanu, D.; Alsaedi, A. Analysis of time-fractional Hunter–Saxton equation: A model of neumatic liquid crystal. *Open Phys.* **2016**, *14*, 145–149. [\[CrossRef\]](#)
- Chen, A. Multi-kink solutions and soliton fission and fusion of the Sharma–Tasso–Olver equation. *Phys. Lett. A* **2012**, *734*, 2340–2345. [\[CrossRef\]](#)
- Sirisubtawee, S.; Koonprasert, S.; Sungnol, S. New exact solutions of the conformable space-time Sharma–Tasso–Olver equation using two reliable methods. *Symmetry* **2020**, *12*, 644. [\[CrossRef\]](#)
- Sheikh, M.A.N.; Taher, M.A.; Hossain, M.M.; Akter, S.; Harun-Or-Rashid. Variable coefficient exact solution of Sharma–Tasso–Olver model by enhanced modified simple equation method. *Partial Differ. Equ. Appl. Math.* **2023**, *7*, 100527. [\[CrossRef\]](#)
- Wazwaz, A. A sine-cosine method for handling nonlinear wave equations. *Math. Comput. Model.* **2004**, *40*, 499–508. [\[CrossRef\]](#)
- Bekir, A.; Boz, A. Exact solutions for nonlinear evolution equations using Exp-function method. *Phys. Lett. A* **2008**, *372*, 1619–1625. [\[CrossRef\]](#)
- Pan, J.; Chen, W. A new auxiliary equation method and its application to the Sharma–Tasso–Olver model. *Phys. Lett. A* **2009**, *373*, 3118–3121. [\[CrossRef\]](#)
- Abbasbandy, S.; Ashtiani, M.; Babolian, E. Analytic solution of the Sharma–Tasso–Olver equation by homotopy analysis method. *Z. Nat.forsch.* **2010**, *65*, 285–290. [\[CrossRef\]](#)
- He, J.; Elagan, S.; Li, Z. Geometrical explanation of the fractional complex transform and derivative chain rule for fractional calculus. *Phys. Lett. A* **2012**, *376*, 257–259. [\[CrossRef\]](#)
- Xue, B.; Wu, C.-M. Conservation laws and Darboux transformation for Sharma–Tasso–Olver equation. *Commun. Theor. Phys* **2012**, *58*, 317. [\[CrossRef\]](#)
- Shang, Y.; Huang, Y.; Yuan, W. Bäcklund transformations and abundant exact explicit solutions of the Sharma–Tasso–Olver equation. *Appl. Math. Comput.* **2011**, *217*, 7172–7183. [\[CrossRef\]](#)
- He, Y.; Li, S.; Long, Y. Exact solutions to the Sharma–Tasso–Olver equation by using improved  $G'/G$ -expansion method. *J. Appl. Math.* **2013**, *2013*, 247234. [\[CrossRef\]](#)
- Rahman, N.; Alam, M.; Roshid, H.; Akter, S.; Akbar, M. Application of  $(-\phi(\xi))$ -expansion method to find the exact solutions of Sharma–Tasso–Olver equation. *Afr. J. Math. Comput. Sci. Res.* **2014**, *7*, 1–6.
- Zhe, Z.; Li, D. The modified multiple  $(G'/G)$ -expansion method and its application to Sharma–Tasso–Olver equation. *Pramana J. Phys.* **2014**, *83*, 95–105. [\[CrossRef\]](#)
- Rawashdeh, M. An efficient approach for time-fractional damped Burger and time-Sharma–Tasso–Olver equations using the FRDTM. *Appl. Math. Inf. Sci.* **2015**, *9*, 1239–1246.
- Alhakim, L.; Moussa, A. The improved  $\exp(-\phi(\xi))$  fractional expansion method and its application to nonlinear fractional Sharma–Tasso–Olver equation. *J. Appl. Comput. Math.* **2017**, *6*, 360.
- Bibi, S.; Mohyud-Din, S.T.; Khan, U.; Ahmed, N. Khater method for nonlinear Sharma Tasso-Olever (STO) equation of fractional order. *Results Phys.* **2017**, *7*, 4440–4450. [\[CrossRef\]](#)
- Gomez, C.; Hernandez, J. Traveling wave solutions for Burgers–Sharma–Tasso–Olver equation with variable coefficients: The improved tanh-coth method vs. exp. function method. *J. Math. Anal.* **2017**, *11*, 825–831. [\[CrossRef\]](#)
- Rezazadeh, H.; Khodadad, F.S.; Manafian, J. New structure for exact solutions of nonlinear time fractional Sharma–Tasso–Olver equation via conformable fractional derivative. *Appl. Appl. Math.* **2017**, *12*, 405–414.
- Butt, A.R.; Zaka, J.; Akül, A. New structures for exact solution of nonlinear fractional Sharma–Tasso–Olver equation by conformable fractional derivative. *Results Phys.* **2023**, *50*, 106541. [\[CrossRef\]](#)
- Fang, T.; Wang, Y.H. Interaction solutions for a dimensionally reduced Hirota bilinear equation. *Comput. Math. Appl.* **2018**, *76*, 1476–1485. [\[CrossRef\]](#)
- Hao, X.; Liu, Y.; Li, Z.; Ma, W.X. Painlevé analysis, soliton solutions and lump-type solutions of the  $(3+1)$ -dimensional generalized KP equation. *Comput. Math. Appl.* **2019**, *77*, 724–730. [\[CrossRef\]](#)



31. Kang, Z.; Xia, T.; Ma, W. Abundant multi wave solutions to the  $(3 + 1)$ -dimensional Sharma-Tasso-Olver-like equation. *Proc. Rom. Acad. Ser. A* **2019**, *20*, 115–122.
32. El-Rashidy, K. New traveling wave solutions for the higher Sharma-Tasso-Olver equation by using extension exponential rational function method. *Results Phys.* **2020**, *17*, 103066. [\[CrossRef\]](#)
33. Li, L.; Wang, M.; Zhang, J. The solutions of initial (-boundary) value problems for Sharma-Tasso-Olver equation. *Mathematics* **2022**, *10*, 441. [\[CrossRef\]](#)
34. Zhou, Y.; Zhuang, J. Dynamics and exact traveling wave solutions of the Sharma–Tasso–Olver–Burgers equation. *Symmetry* **2022**, *14*, 1468. [\[CrossRef\]](#)
35. Han, T.; Jiang, Y. Bifurcation, chaotic pattern and traveling wave solutions for the fractional Bogoyavlenskii equation with multiplicative noise. *Phys. Scr.* **2024**, *99*, 035207. [\[CrossRef\]](#)
36. Aniga, A.; Ahmad, J. Soliton solution of fractional Sharma-Tasso-Olver equation via an efficient  $(G'/G)$ -expansion method. *Ain Shams Eng. J.* **2022**, *13*, 101528. [\[CrossRef\]](#)
37. Yang, S. Traveling wave solution for Sharma–Tasso–Olver–Burgers (STOB) equation by the  $(G'/G)$ -expansion method. *Sch. J. Phys. Math. Stat.* **2022**, *9*, 46–51. [\[CrossRef\]](#)
38. Khalil, T.A.; Badra, N.; Ahmed, H.M.; Rabie, W.B. Optical solitons and other solutions for coupled system of nonlinear Biswas–Milovic equation with Kudryashov’s law of refractive index by Jacobi elliptic function expansion method. *Optik* **2022**, *253*, 168540. [\[CrossRef\]](#)
39. Ozisik, M.; Secer, A.; Bayram, M. On solitary wave solutions for the extended nonlinear Schrödinger equation via the modified F-expansion method. *Opt. Quantum Electron.* **2023**, *55*, 215. [\[CrossRef\]](#)
40. Gu, M.; Peng, C.; Li, Z. Traveling wave solution of  $(3 + 1)$ -dimensional negative-order KdV-Calogero-Bogoyavlenskii-Schiff equation. *AIMS Math.* **2024**, *9*, 6699–6708. [\[CrossRef\]](#)
41. Yépez-Martínez, H.; Gómez-Aguilar, J.; Baleanu, D. Beta-derivative and sub-equation method applied to the optical solitons in medium with parabolic law nonlinearity and higher order dispersion. *Optik* **2018**, *155*, 357–365. [\[CrossRef\]](#)
42. Rezazadeh, H.; Inc, M.; Baleanu, D. New solitary wave solutions for variants of  $(3 + 1)$ -dimensional Wazwaz-Benjamin-Bona-Mahony equations. *Front. Phys.* **2020**, *8*, 332. [\[CrossRef\]](#)
43. Asjad, M.; Inc, M.; Iqbal, I. Exact solutions for new coupled Konno-Oono equation via Sardar subequation method. *Opt. Quantum Electron.* **2022**, *54*, 798.
44. Rahman, H.; Iqbal, I.; Aiadi, S.S.; Mlaiki, N.; Saleem, M. Soliton solutions of Klein–Fock–Gordon equation using Sardar subequation method. *Mathematics* **2022**, *10*, 3377. [\[CrossRef\]](#)
45. Rahman, H.; Asjad, M.; Munawar, N.; Parvaneh, F.; Muhammad, T.; Hamoud, A.; Emadifar, H.; Hamaslh, F.; Azizi, H.; Khademi, M. Traveling wave solutions in the Boussineq equation via Sardar subequation technique. *AIMS Math.* **2022**, *7*, 11134–11149. [\[CrossRef\]](#)
46. Cinar, M.; Secer, A.; Ozisik, M.; Bayram, M. Derivation of optical solitons of dimensionless Fokas-Lenells equation with perturbation term using Sardar subequation method. *Opt. Quantum Electron.* **2022**, *54*, 402. [\[CrossRef\]](#)
47. Alsharidi, A.K.; Bekir, A. Discovery of new exact wave solutions to the M-fractional complex three coupled Maccari’s system by Sardar subequation scheme. *Symmetry* **2023**, *15*, 1567. [\[CrossRef\]](#)
48. Khan, M.I.; Farooq, A.; Nisar, K.S.; Shah, N.A. Unveiling new exact solutions of the unstable nonlinear Schrödinger equation using the improved modified Sardar subequation method. *Results Phys.* **2024**, *59*, 107593. [\[CrossRef\]](#)
49. Pleumpreedaporn, C.; Pleumpreedaporn, S.; Moore, E.J.; Sirisubtawee, S.; Sungnol, S. Novel exact traveling wave solutions for the  $(2 + 1)$ -dimensional Boiti–Leon–Manna–Pempinelli equation with Atangana’s space and time beta-derivatives via the Sardar subequation method. *Thai J. Math* **2024**, *22*, 1–18.
50. Hussain, R.; Imtiaz, A.; Rasool, T.; Rezazadeh, H.; Inc, M. Novel exact and solitary solutions of conformable Klein–Gordon equation via Sardar subequation method. *J. Ocean Eng. Sci.* **2022**, *in press*. [\[CrossRef\]](#)
51. Atangana, A.; Baleanu, D. New fractional derivatives with nonlocal and non-singular kernel: Theory and application to heat transfer model. *Therm. Sci.* **2016**, *20*, 763–769. [\[CrossRef\]](#)
52. Syam, M.I.; Al-Refai, M. Fractional Differential Equations with Atangana-Baleanu Fractional Derivative: Analysis and Applications. *Chaos Soliton Fract.* **2019**, *2*, 100013. [\[CrossRef\]](#)
53. Uddin, M.F.; Hafez, M.G.; Hammouch, Z.; Baleanu, D. Periodic and rogue waves for Heisenberg models of ferromagnetic spin chains with fractional beta derivative evolution and obliqueness. *Waves Random Complex Media* **2021**, *31*, 2135–2149. [\[CrossRef\]](#)
54. Hosseini, K.; Mirzazadeh, M.; Gómez-Aguilar, J. Soliton solutions of the Sasa-Satsuma equation in the monomode optical fibers including the beta-derivatives. *Optik* **2020**, *224*, 165425. [\[CrossRef\]](#)
55. Rafiq, M.; Majeed, A.; Inc, M.; Kamran, M.; Baleanu, D. New traveling wave solutions for space-time fractional modified equal width equation with beta derivative. *Phys. Lett. A* **2021**, *446*, 128281. [\[CrossRef\]](#)
56. Ozkan, E. New exact solutions of some important nonlinear fractional partial differential equations with beta derivative. *Fractal Fract.* **2022**, *6*, 173. [\[CrossRef\]](#)
57. Akbulut, A.; Islam, S. Study on the Biswas–Arshed equation with the beta time derivative. *Int. J. Appl. Comput. Math.* **2022**, *8*, 167. [\[CrossRef\]](#)
58. Podlubny, I. *Fractional Differential Equations*; Academic Press: New York, NY, USA, 1999.
59. Caputo, M. Linear model of dissipation whose Q is almost frequency independent. II. *Geophys. J. Int.* **1967**, *13*, 529–539. [\[CrossRef\]](#)

60. Caputo, M.; Fabrizio, M. A new definition of fractional derivative without singular kernel. *Prog. Fract. Differ. Appl.* **2015**, *1*, 73–85. [[CrossRef](#)]
61. Kilbas, A. Hadamard-type fractional calculus. *J. Korean Math. Soc.* **2001**, *38*, 1191–1204.
62. Hilfer, R. *Applications of Fractional Calculus in Physics*; World Scientific: Singapore, 2000.
63. Ahmed, I.; Kumam, P.; Jarad, F.; Borisut, P.; Jirakitpuwapat, W. On Hilfer generalized proportional fractional derivative. *Adv. Differ. Equ.* **2020**, *2020*, 329. [[CrossRef](#)]
64. Katugampola, U.N. A new approach to generalized fractional derivatives. *Bull. Math. Anal. Appl.* **2014**, *6*, 1–15.
65. Hattaf, K. On the stability and numerical scheme of fractional differential equations with application to biology. *Computation* **2022**, *10*, 97. [[CrossRef](#)]
66. Khalid, H. A new class of generalized fractal and fractal-fractional derivatives with non-singular kernels. *Fractal Fract.* **2023**, *7*, 395. [[CrossRef](#)]
67. Hanif, A.; Butt, A.I.K.; Ismaeel, T. Fractional optimal control analysis of COVID-19 and dengue fever co-infection model with Atangana-Baleanu derivative. *AIMS Math.* **2024**, *9*, 5171–5203. [[CrossRef](#)]
68. Malingam, P.; Wongsasinchai, P.; Sirisubtawee, S.; Koonprasert, S. Exact Solutions of the Paraxial Wave Dynamical Model in Kerr Media with Truncated M-fractional Derivative using the  $(G'/G, 1/G)$ -Expansion Method. *WSEAS Trans. Syst. Control* **2023**, *18*, 498–512. [[CrossRef](#)]

**Disclaimer/Publisher's Note:** The statements, opinions and data contained in all publications are solely those of the individual author(s) and contributor(s) and not of MDPI and/or the editor(s). MDPI and/or the editor(s) disclaim responsibility for any injury to people or property resulting from any ideas, methods, instructions or products referred to in the content.